www.elsevier.nl/locate/jorganchem

Journal of Organometallic Chemistry 622 (2001) 210–220

Synthesis and electrochemical properties of organometallic macrocyclic crown ethers containing redox-active tetrahedral $Mo_2Fe(\mu_3\text{-}S)$ cluster cores. Crystal structures of $[Mo_2Fe(\mu_3\text{-}S)(CO)_7][\eta^5\text{-}C_5H_4CH_2(CH_2OCH_2)_n\ CH_2C_5H_4\text{-}\eta^5]$ $(n=1-3)$

Li-Cheng Song [a,*], Dian-Shun Guo [a], Qing-Mei Hu [a], Fu-Hai Su [a], Jie Sun [b], Xiao-Ying Huang [c]

[a] *Department of Chemistry, State Key Laboratory of Elemento-Organic Chemistry, Nankai University, Tianjin 300071, People's Republic of China*
[b] *Laboratory of Organometallic Chemistry, Shanghai 200032, People's Republic of China*
[c] *Laboratory of Structural Chemistry, Fuzhou 350002, People's Republic of China*

Received 17 October 2000; received in revised form 22 November 2000; accepted 25 November 2000

Abstract

The self-assembly cyclization reactions of the ether chain-bridged dicyclopentadienyl Mo/Na salts $[NaMo(CO)_3]_2[\eta^5\text{-}C_5H_4CH_2(CH_2OCH_2)_nCH_2C_5H_4\text{-}\eta^5]$ (**Ia-d**, $n = 1$–4) with the same chain-bridged dicyclopentadienyl double clusters $[MoCoFe(\mu_3\text{-}S)(CO)_8]_2[\eta^5\text{-}C_5H_4CH_2(CH_2OCH_2)_nCH_2C_5H_4\text{-}\eta^5]$ (**Iia–d**, $n = 1$–4) have been found, depending on the lengths of the bridged ether chains in starting materials **I** and **II**, to give several different types of novel organometallic macrocyclic crown ethers. While reaction of the Mo/Na salts (**I**, $n=1$, 4) with double clusters (**II**, $n=1$, 4) produced single $Mo_2Fe(\mu_3\text{-}S)$ cluster crown ethers $[Mo_2Fe(\mu_3\text{-}S)(CO)_7][\eta^5\text{-}C_5H_4CH_2(CH_2OCH_2)_n\ CH_2C_5H_4\text{-}\eta^5]$ (**IIIa**, $n=1$; **IIId**, $n=4$), the Mo/Na salts (**I**, $n=2$, 3) reacted with double clusters (**II**, $n=2$, 3) to afford single, double and triple $Mo_2Fe(\mu_3\text{-}S)$ cluster crown ethers $[Mo_2Fe(\mu_3\text{-}S)(CO)_7]_m[\eta^5\text{-}C_5H_4CH_2(CH_2OCH_2)_nCH_2\ C_5H_4\text{-}\eta^5]_m$ (**IIIb**, $n=2$, $m=1$; **IIIc**, $n=3$, $m=1$; **IVb**, $n=2$, $m=2$; **IVc**, $n=3$, $m=2$; **Vb**, $n=2$, $m=3$; **Vc**, $n=3$, $m=3$), respectively. While structures of **IIIa**–**d**, **IVb**,**c** and **Vb**,**c** were characterized fully by elemental analyses, IR, ^{1}H-NMR and FAB-MS spectrocopies, those of **IIIa**–**c** were further confirmed by X-ray diffraction techniques. In addition, the electrochemical properties of **IIIa**–**d**, **IVb**,**c** and **Vb**,**c** have been studied using cyclic voltammetry.

Keywords: Molybdenum; Iron; Cobalt; Crown ether; Crystal structures

1. Introduction

The crown ethers, since their discovery in 1967 [1], have been receiving considerable attention, primarily because they have unique structures, valuable properties, and particularly the important applications in various fields such as the catalytic synthesis, ion and molecular recognitions, and sensor technology, etc. [2–6]. Among crown ethers, the organometallic ones that combine both crown ether and organometallic structural units are of great interest, since in such crown ethers the affinity of the crown ether subunit toward metal complexation can be regulated by the oxidation state of the redox-active metal centers. However, until now, only a few of organometallic crown ethers which contain transition metal cluster cores have been reported [7], although numerous other organometallic crown ethers have been prepared and studied, such as those containing transition metals Ti [8], Zr [9], Cr [10], Mo [11], W [12], Mn [13], Re [14], Fe [15], Ru [16], Co [17] and Rh [18] as redox-active centers. On the basis of

---

* Corresponding author. Fax: +86-22-23504853.
E-mail address: lcsong@public.tpt.tj.cn (L.-C. Song).

PII: S0022-328X(00)00915-3

our preliminary report on organometallic cluster crown ethers [7], we wish to further report the detailed results obtained from a systematic study of such cluster crown ethers, including their synthetic procedures, spectroscopic and electrochemical properties, as well as three crystal structures determined by X-ray diffraction techniques.

2. Results and discussion

2.1. Self-assembly cyclization reactions of ***Ia–d*** with ***IIa–d***. Synthesis and characterization of ***IIIa–d***, ***IVb***,***c*** and ***Vb***,***c***

In a previous communication [7], we reported that reaction of the polyether chain-bridged dicyclopentadienyl Mo/Na salt $[NaMo(CO)_3]_2[\eta^5\text{-}C_5H_4CH_2(CH_2OCH_2)_n CH_2C_5H_4\text{-}\eta^5]$ (**Ic**, $n = 3$) with the same chain-bridged dicyclopentadienyl double cluster $[MoCoFe(\mu_3\text{-}S)(CO)_8]_2[\eta^5\text{-}C_5H_4CH_2 (CH_2 OCH_2)_nCH_2C_5H_4\text{-}\eta^5]$ (**IIc**, $n = 3$) in THF at reflux gave not only the expected cyclization product $[Mo_2Fe(\mu_3\text{-}S)(CO)_7]_2[\eta^5\text{-}C_5H_4CH_2(CH_2OCH_2)_nCH_2C_5H_4\text{-}\eta^5]_2$ (**IVc**, $n = 3$), but also afforded two unexpected cyclization products $[Mo_2Fe(\mu_3\text{-}S)(CO)_7][\eta^5\text{-}C_5H_4CH_2(CH_2OCH_2)_nCH_2C_5H_4\text{-}\eta^5]$ (**IIIc**, $n = 3$) and $[Mo_2Fe (\mu_3\text{-}S)(CO)_7]_3[\eta^5\text{-}C_5H_4 CH_2(CH_2OCH_2)_nCH_2C_5H_4\text{-}\eta^5]_3$ (**Vc**, $n = 3$) (Scheme 1). Interestingly, we further found that this novel cyclization reaction can be markedly influenced by the lengths of the bridged ether chains in starting materials **Ia–d** and **IIa–d**, to give not always the three types of cyclization products. For example, while **Ib** ($n = 2$) reacted with **IIb** ($n = 2$) under similar conditions to produce three types of cyclization products $[Mo_2Fe(\mu_3\text{-}S)(CO)_7][\eta^5\text{-}C_5H_4CH_2(CH_2O CH_2)_nCH_2C_5H_4\text{-}\eta^5]$ (**IIIb**, $n = 2$), $[Mo_2Fe(\mu_3\text{-}S)(CO)_7]_2[\eta^5\text{-}C_5H_4CH_2(CH_2OCH_2)_nCH_2 C_5H_4\text{-}\eta^5]_2$ (**IVb**, $n = 2$) and $[Mo_2Fe(\mu_3\text{-}S)(CO)_7]_3[\eta^5\text{-}C_5H_4CH_2(CH_2OCH_2)_nCH_2C_5H_4\text{-}\eta^5]_3$ (**Vb**, $n = 2$), reaction of **Ia** ($n = 1$) with **IIa** ($n = 1$) or **Id** ($n = 4$) with **IId** ($n = 4$) gave only the first type of cyclization products $[Mo_2Fe(\mu_3\text{-}S)(CO)_7][\eta^5\text{-}C_5H_4CH_2(CH_2OCH_2)_n CH_2C_5H_4\text{-}\eta^5]$ (**IIIa**, $n = 1$; **IIId**, $n = 4$), without any appreciable amounts of the other two types of cyclization products **IVa** and **Va** ($n = 1$) or **IVd** and **Vd** ($n = 4$) being isolated (Scheme 1).

It should be noted that the cyclization reactions mentioned above were conveniently carried out in one-pot, starting from disodium salts $Na_2[\eta^5\text{-}C_5H_4 CH_2(CH_2OCH_2)_nCH_2C_5H_4\text{-}\eta^5]$ ($n = 1$–4) and $Mo(CO)_6$, followed by treatment of the intermediates **Ia–d** with double clusters **IIa–d** [19,20]. Products **IIIa–d**, **IVb**,**c** and **Vb**,**c** are air-stable and red-brown to black solids, which have been characterized by elemental analysis, IR, ^{1}H-NMR and FAB-MS specroscopies, as well as for **IIIa–c** by X-ray diffraction analyses.

The IR spectra of **IIIa–d**, **IVb**,**c** and **Vb**,**c** showed several absorption bands in the range 2034–1821 cm^{-1} for their carbonyls attached to transition metals and one absorption band in the range 1126–1102 cm^{-1} for their bridged ether chain functionalities. Whereas the ^{1}H-NMR spectra of single cluster crown ethers **IIIa–d** displayed two multiplets in the ranges 2.57–3.10 and 3.47–3.79 ppm for α-CH$_2$ attached to Cp rings and

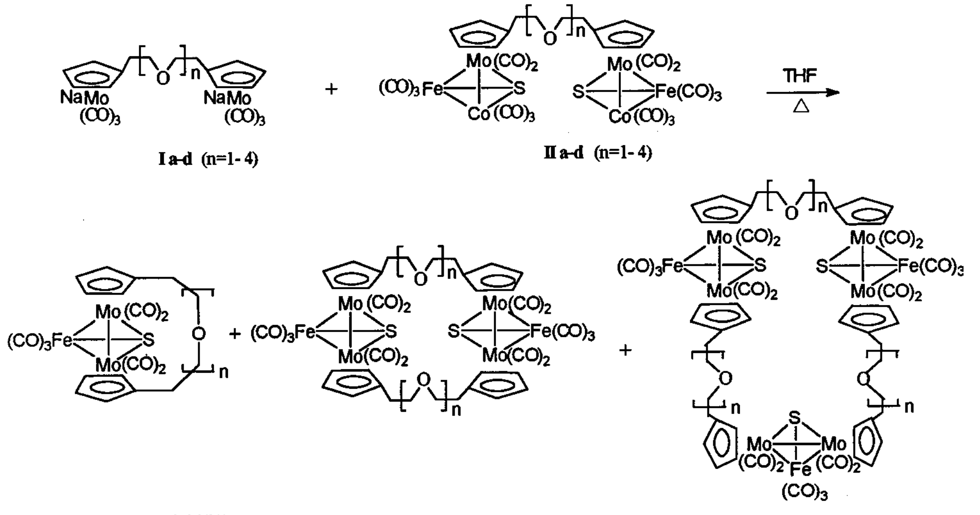

n		yield(%)
1	**IIIa**	10
2	**IIIb**	21
3	**IIIc**	25
4	**IIId**	17

	yield(%)
IVa	—
IVb	15
IVc	17
IVd	—

	yield(%)
Va	—
Vb	5
Vc	11
Vd	—

Scheme 1.

Table 1
FAB-MS data of cluster crown ethers (Mo^{98}, S^{32}, Fe^{56})

Cluster	Ion	*m*/*z* (rel. intensity, %)	Cluster	Ion	*m*/*z* (rel. intensity, %)
IIIa	M^{+}	680(66)	**IVb**	$M^{+}-7H--O$	1413(18)
	$M^{+}-3H$	677(87)		$M^{+}-6H-4CO$	1343(67)
	$M^{+}-3H-CO$	649(100)		$M^{+}-7H-9CO$	1189(53)
	$M^{+}-4H-2CO$	620(72)		$M^{+}-6H-14CO$	1050(100)
	$M^{+}-4H-3CO$	592(84)			
	$M^{+}-4H-4CO$	564(58)			
	$M^{+}-4H-5CO$	536(91)			
	$M^{+}-4H-6CO$	508(77)			
	$M^{+}-5H-7CO$	479(49)			
IIIb	M^{+}	724(35)	**IVc**	M^{+}	1356(15)
	$M^{+}-3H$	721(49)		$M^{+}-H-3CO$	1451(91)
	$M^{+}-3H-CO$	693(4)		$M^{+}-9CO$	1284(35)
	$M^{+}-4H-2CO$	664(47)		$M^{+}-6H-11CO$	1222(50)
	$M^{+}-4H-3CO$	636(16)		$M^{+}-6H-12CO$	1194(23)
	$M^{+}-4H-5CO$	580(100)		$M^{+}-6H-13CO$	1166(25)
	$M^{+}-4H-6CO$	552(45)		$M^{+}-6H-14CO$	1138(84)
	$M^{+}-5H-7CO$	523(14)			
IIIc	M^{+}	768(14)	**Vb** [a]	M^{+}	2160(60)
	$M^{+}-3H$	765(35)		$M^{+}-3CO$	2076(65)
	$M^{+}-3H-CO$	737(2)		$M^{+}-9CO$	1908(15)
	$M^{+}-4H-2CO$	708(3)		$M^{+}-20CO$	1600(34)
	$M^{+}-4H-3CO$	680(32)			
	$M^{+}-4H-5CO$	624(100)			
	$M^{+}-4H-6CO$	596(21)			
	$M^{+}-5H-7CO$	567(6)			
IIId	M^{+}	812(28)	**Vc** [a]	M^{+}	2292(51)
	$M^{+}-3H$	809(44)		$M^{+}-CO$	2264(18)
	$M^{+}-4H-3CO$	724(59)		$M^{+}-3CO$	2208(58)
	$M^{+}-4H-5CO$	668(100)		$M^{+}-20CO$	1732(30)
	$M^{+}-4H-6CO$	640(12)			

[a] *m*/*z* (^{96}Mo) for these clusters.

their neighboring β-CH_2 (for **IIIb**–**d** the latter range includes the other CH_2 resonances), those of double and triple cluster crown ethers **IVb**,**c** and **Vb**,**c** exhibited two singlets in the ranges 2.63–2.65 and 3.59–3.62 ppm for their α-CH_2 and corresponding β-CH_2 groups, respectively. It is believed that such two different ^{1}H-NMR patterns for α-CH_2 and β-CH_2 in the single, double and triple cluster crown ethers might be attributed to the restricted rotation of the bridged ether chains in smaller rings of the single cluster crown ethers and the capable free rotation of the bridged ether chains in the larger rings of the double and triple cluster crown ethers [7]. In addition, while the ^{1}H-NMR spectra of single cluster crown ethers **IIIa**–**d** showed one singlet, one triplet or two singlets in the range 4.97–5.20 ppm assigned to H^2/H^5 protons of the Cp rings and two singlets in the range 5.20–5.65 ppm assigned to H^3/H^4 protons of the Cp rings, those of double and triple cluster crown ethers **IVb**,**c** and **Vb**,**c** displayed two singlets, four singlets, or one multiplets in the range 5.15–5.31 ppm assigned to H^2/H^5 and H^3/H^4 protons of the Cp rings, respectively. That is, the ^{1}H-NMR patterns of the substituted Cp rings of crown ethers **IIIa**–**d**, **IVb**,**c** and **Vb**,**c** are very complicated, which is consistent with the fact that ^{1}H-NMR spectra of a monosubstituted cyclopentadienyl ring in organometallic clusters vary greatly in complexity such as a singlet, an A_2B_2 or A_2BB' pattern or a multiplet, mainly depending on the nature of the substituent and chirality of the molecule [21]. The FAB-MS data of **IIIa**–**d**, **IVb**,**c** and **Vb**,**c** listed in Table 1, show their respective molecular ions M^+(except **IVb**) and corresponding fragment ions by loss of a given number of H atoms and/or CO ligands, consistent with their macrocyclic structures shown in Scheme 1. Finally, the elemental analyses for transition metals performed on a plasma atom emission spectrometer also support those macrocyclic structures, since they indicated no Co atom present and the stoichiometry of Mo:Fe is 2:1.

2.2. Crystal structures of *IIIa*–*c*

The molecular structures of cluster crown ethers **IIIa**–**c** have been confirmed by X-ray diffraction analyses. The X-ray diffraction analyses showed that while **IIIa**,**b** each have one crystallographically independent molecule in their unit cells, **IIIc** has two independent molecules A and B in its unit cell with very similar crystallographic parameters. So, while the molecular structures of **IIIa** and **IIIb** are shown in Figs. 1 and 2, for simplicity only one of the two very similar crystallographically independent molecules of **IIIc**, i.e. molecule A is given in Fig. 3. In addition, for the same season only some of the bond lengths and angles of molecule A of **IIIc** are listed in Table 2, along with corresponding those of **IIIa** and **IIIb**.

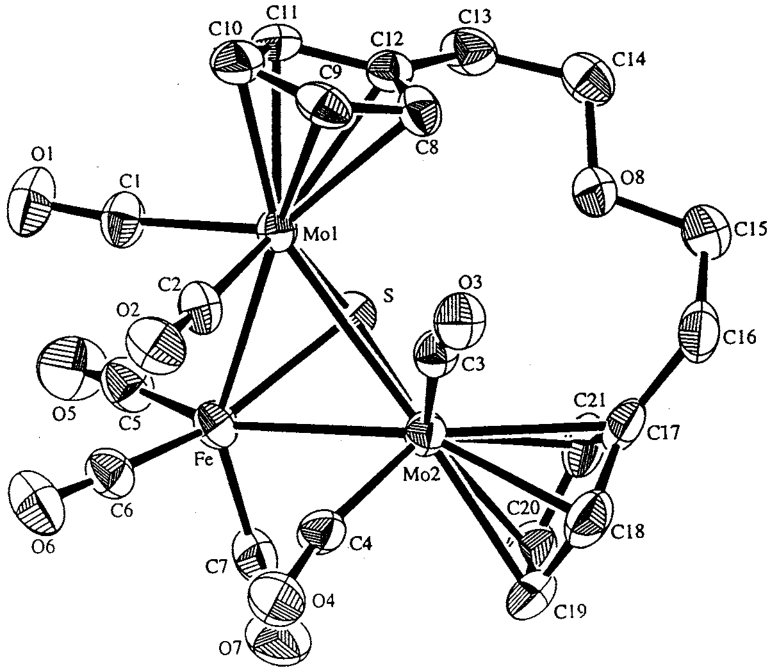

Fig. 1. ORTEP plot of **IIIa** with the atom labeling scheme.

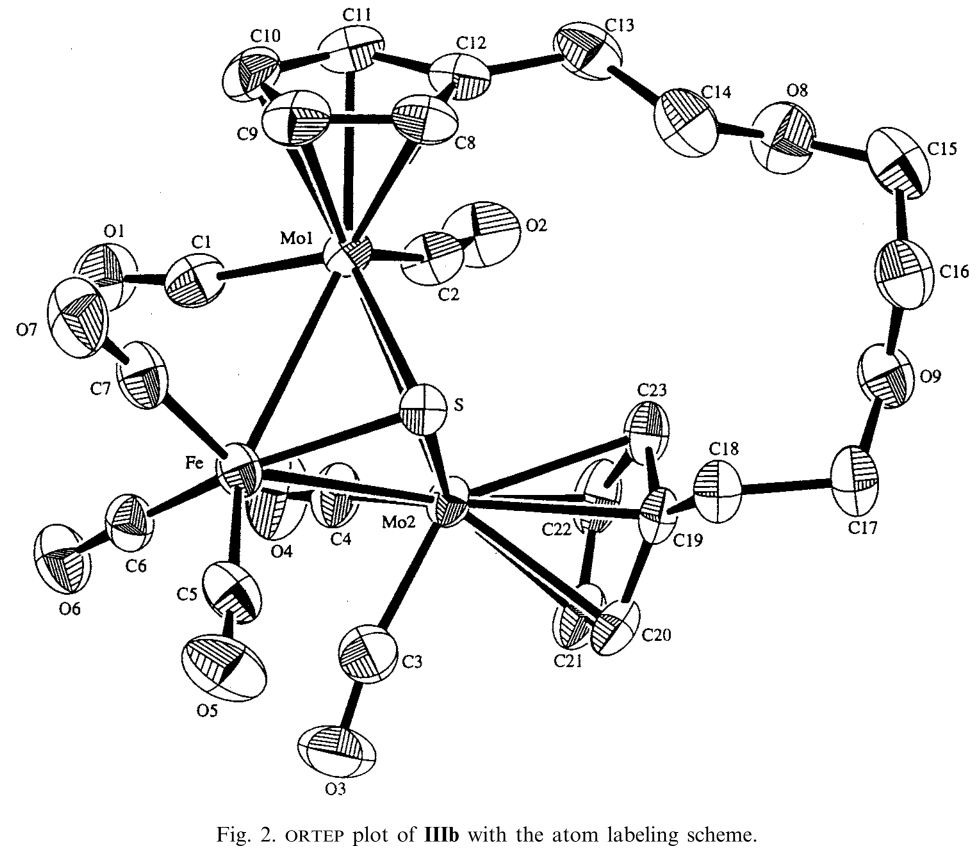

Fig. 2. ORTEP plot of **IIIb** with the atom labeling scheme.

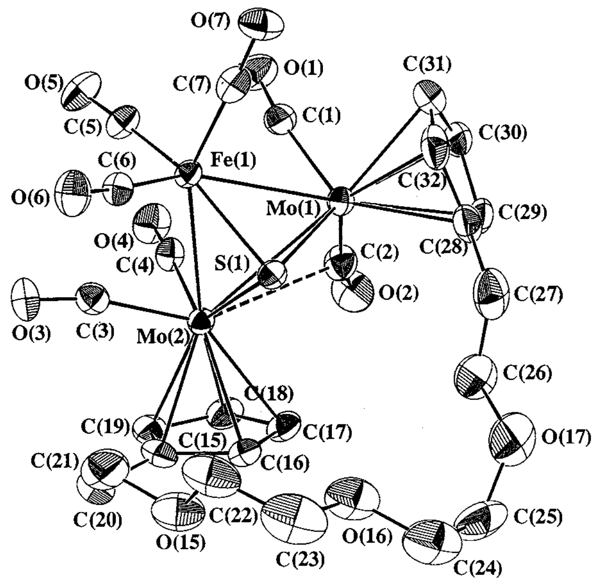

Fig. 3. ORTEP plot of **IIIc** with the atom labeling scheme.

Table 2
Selected bond lengths (Å) and bond angles (°) for **IIIa–c**

	IIIa	IIIb	IIIc
Bond lengths			
Mo(1)–Mo(2)	3.053(1)	3.0534(9)	3.042(1)
Mo(1)–S	2.368(2)	2.377(1)	2.366(2)
Mo(2)–S	2.379(2)	2.369(1)	2.370(2)
Mo(1)–Fe	2.839(1)	2.804(1)	2.796(1)
Mo(2)–Fe	2.804(2)	2.819(1)	2.825(1)
Fe–S	2.197(2)	2.197(2)	2.196(2)
Bond angles			
Mo(2)–Mo(1)–Fe	56.69(3)	57.33(3)	57.69(3)
Mo(1)–Mo(2)–Fe	57.81(3)	56.89(3)	56.78(3)
Mo(1)–Fe–Mo(2)	65.49(3)	65.78(2)	65.53(3)
Mo(1)–Mo(2)–S	49.81(5)	50.08(3)	49.98(5)
Mo(2)–Mo(1)–S	50.15(5)	49.83(3)	50.10(5)
Mo(1)–S–Mo(2)	80.04(7)	80.08(4)	79.92(6)
Fe–Mo(1)–S	48.88(5)	49.34(4)	49.49(5)
Fe–Mo(2)–S	49.32(5)	49.19(4)	49.05(5)
Mo(1)–Fe–S	54.29(6)	55.16(4)	55.01(6)
Mo(2)–Fe–S	55.23(6)	54.68(3)	54.62(6)
Mo(1)–S–Fe	76.83(7)	75.50(5)	75.50(7)
Mo(2)–S–Fe	75.45(7)	76.13(5)	76.33(7)

Table 3
Some dihedral angles (°) for **IIIa–c**

	IIIa [a]	IIIb [b]	IIIc [c]
Mo(1)FeMo(2)/Cp(1)	76.8	109.1	104.4
Mo(1)FeMo(2)/Cp(2)	69.3	74.4	71.1
Cp(1)/Cp(2)	104.9	72.8	70.8

[a] Cp(1): C_8–C_{12}, Cp(2): C_{17}–C_{21}.

[b] Cp(1): C8–C12, Cp(2): C19–C23.

[c] Cp(1): C(15)–C(19), Cp(2): C(28)–C(32).

As seen in Figs. 1–3, **IIIa–c** consist of a distorted tetrahedral $Mo_2Fe(\mu_3\text{-}S)$ cluster core, which carries one ether chain-bridged dicyclopentadienyl ligand coordinated to two Mo atoms, one set of three CO ligands attached to Fe atom and two sets of two CO ligands attached to two Mo atoms, respectively. Actually, **IIIa–c** belong to the same type of macrocyclic cluster crown ethers with different lengths of the bridging ether chain. For any of the crown ethers with a given length of the bridging ether chain, for example, for **IIIa** the molecule could be viewed as a ring size-varied crown ether, depending on which carbon atoms of the two Cp rings C8-through-C12 and C17-through-C21 and which metal atoms of Mo1, Mo2 and Fe are involved in counting the cyclic size of the crown ether containing sulfur and oxygen atoms.

As can be seen from Table 2, the bond lengths and bond angles associated with the cluster cores of **IIIa–c** are very similar and even identical. That is, **IIIa–c** possess a tetrahedral $Mo_2Fe(\mu_3\text{-}S)$ cluster core with almost identical geometric parameters. In fact, such a kind of cluster core is also contained in previously reported simple clusters, such as $(\eta^5\text{-}RC_5H_4)_2Mo_2Fe(\mu_3\text{-}S)(CO)_9$ (R = H [22], COMe [23], CO_2Me [23]). The dihedral angles between the Cp rings (Table 3) have varied markedly from **IIIa** to **IIIc**, apparently due to the presence of different lengths of the ether chain substituents. It is worth to note that the different dihedral angles between Mo(1)FeMo(2) and Cp(1) and between Mo(1)FeMo(2) and Cp(2) can make the two α-hydrogen atoms attached to C13 or C16 (**IIIa**), C13 or C18 (**IIIb**) and C(20) or C(27) (**IIIc**), and those β-hydrogen atoms attached to C14 or C15 (**IIIa**), C14 or C17 (**IIIb**) and C(21) or C(26) (**IIIc**) magnetically inequivalent and thus to give the complicated ^{1}H-NMR spectral patterns as described above.

Finally, it should be pointed out that among the seven carbonyls for each of **IIIa–c**, while the three carbonyls attached to Fe and one carbonyl attached to Mo are terminal, the other three attached to Mo are semibridging. This is because the asymmetry parameters α for the latter three carbonyls fall within the range $0.1 \le \alpha \le 0.6$ [24]. The semibridging carbonyls of **IIIa–c** are shown in Table 4, along with some of related data. So, the existence of both terminal and semibridging carbonyls confirmed by X-ray diffraction is in good agreement with the fact that the IR spectra of **IIIa–c** showed absorption bands ranging from 2034–1821 cm^{-1}.

2.3. How to understand the formation of the cyclization products

The formation of the three types of cluster crown ethers **IIIa–d**, **IVb,c** and **Vb,c** is not completely understood, so far. However, based on the isolobal analogy principle [25] and the reported isolobal displacement

Table 4
Semibridging CO's for **IIIa–c** [a]

	d_1 (Å)	d_2 (Å)	α
IIIa			
C(1)O(1)	Mo(1)–C(1) 1.995	Fe···C(1) 2.794	0.40
C(3)O(3)	Mo(2)–C(3) 1.946	Mo(1)···C(3) 2.835	0.46
C(4)O(4)	Mo(2)–C(4) 1.962	Fe···C(4) 2.810	0.43
IIIb			
C(1)O(1)	Mo(1)–C(1) 1.974	Fe···C(1) 2.837	0.44
C(2)O(2)	Mo(1)–C(2) 1.934	Mo(2)···C(2) 2.859	0.48
C(3)O(3)	Mo(2)–C(3) 1.978	Fe···C(3) 2.711	0.37
IIIc			
C(1)O(1)	Mo(1)–C(1) 1.980	Fe···C(1) 2.829	0.43
C(2)O(2)	Mo(1)–C(2) 1.960	Mo(2)···C(2) 2.900	0.48
C(3)O(3)	Mo(2)–C(3) 1.970	Fe···C(3) 2.665	0.35

[a] An asymmetric parameter α is defined as $\alpha = d_2 - d_1/d_1$, where d_1 and d_2 are the short and long distances of M–C(O), respectively [24].

modes [21a–c,26], we might suggest a possible pathway, which basically the same as that mentioned in our communication [7], to account for the formation of those types of crown ethers.

According to this suggested pathway (Scheme 2), the bridged Mo/Na salts of type **I** can be converted into their decarbonylated intermediates $\mathbf{m_1}$. Then, while these intermediates react further with double clusters of type **II** through intermolecular single isolobal d^5ML_5/d^5ML_5 displacement to give two molecules of intermediates $\mathbf{m_2}$, their reactions with **II** via intermolecular single isolobal d^5ML_5/d^9ML_3 displacement give intermediates $\mathbf{m_3}$. Furthermore, while $\mathbf{m_2}$ undergoes an intramolecular d^5ML_5/d^9ML_3 single isolobal displacement to give single cluster crown ethers of type **III**, the intramolecular single isolobal d^5ML_5/d^9ML_3 displacement of $\mathbf{m_3}$ affords double cluster crown ethers of type **IV**. If $\mathbf{m_2}$ react with $\mathbf{m_3}$ through intermolecular d^5ML_5/d^9ML_3 single isolobal displacement, then the intermediates $\mathbf{m_4}$ will be produced. Finally, the intramolecular single isolobal d^5ML_5/d^9ML_3 displacement of $\mathbf{m_4}$ yields triple cluster crown ethers of type **V**.

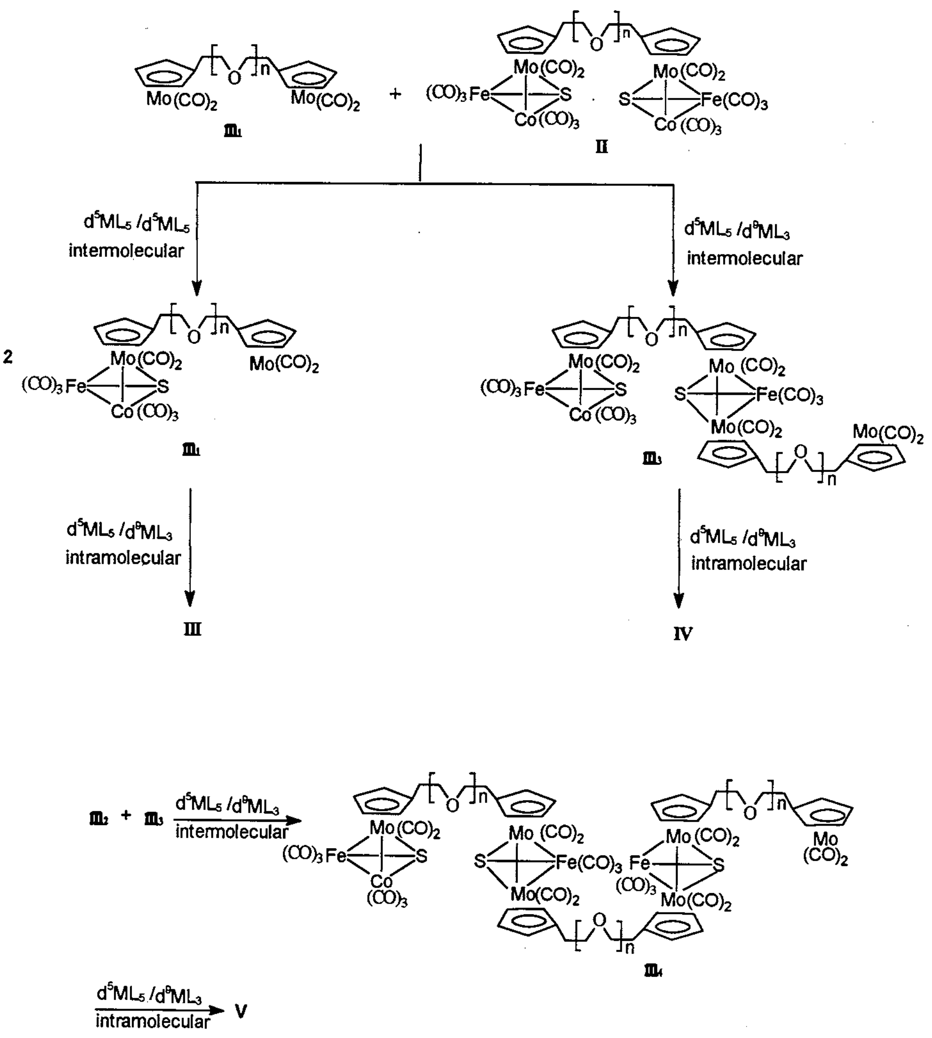

Scheme 2. One possible pathway for production of **III**–**V**.

Table 5
Electrochemical data for **IIIa–d**, **IVb**,**c** and **Vb**,**c** [a]

	E (V)	ΔE (mV)	I_{pc}/I_{pa}		E (V)	ΔE (mV)	I_{pc}/I_{pa}
IIIa	$E_{1/2}+0.62$	91	0.87	**IVb**	$E_{1/2}+0.65$	75	1.00
	$E_{pa1}+0.92$		irr.		$E_{pa1}+1.03$		irr.
	$E_{pa2}+1.11$		irr.		$E_{pc}-1.34$		irr.
	$E_{pc}-1.58$		irr.				
IIIb	$E_{1/2}+0.66$	82	0.81	**IVc**	$E_{1/2}+0.65$	80	0.90
	$E_{pa1}+1.17$		irr.		$E_{pa1}+1.05$		irr.
	$E_{pc}-1.37$		irr.		$E_{pc}-1.43$		irr.
IIIc	$E_{1/2}+0.65$	81	0.99	**Vb**	$E_{1/2}+0.66$	82	1.05
	$E_{pa1}+1.08$		irr.		$E_{pa1}+1.06$		irr.
	$E_{pc}-1.29$		irr.		$E_{pc}-1.41$		irr.
IIId	$E_{1/2}+0.65$	85	0.83	**Vc**	$E_{1/2}+0.66$	78	0.94
	$E_{pa1}+1.07$		irr.		$E_{pa1}+0.99$		irr.
	$E_{pc}-1.46$		irr.		$E_{pc}-1.44$		irr.

[a] Measured in dichloromethane solution containing 0.1 M n-Bu_4NPF_6 as supporting electrolyte. Solutions were ca. 1.0×10^{-3} M in crown ether, and potentials were determined with reference to SCE at room temperature (20 ± 1°C) and scan rate = 100 mV s^{-1}.

However, in order to further account for the fact that the formation of the three types of products considerably depends upon the lengths of the bridged ether chains in starting materials **Ia**–**d** and **IIa**–**d**, we might further suggest that the ring closure steps of $\mathbf{m_2}$–$\mathbf{m_4}$ would be controlled by template effects [27] caused by oxygen atoms in the bridged ether chains and sodium ion Na^+ present in the reaction systems. That is, when $n = 1$ and 4, the template effects for intermediates $\mathbf{m_3}$ and $\mathbf{m_4}$ are too weak for ring closure to give the second and third types of larger macrocyclic crown ethers **IVa**,**d** and **Va**,**d**, whereas when $n = 2$ and 3, the template effects for $\mathbf{m_2}$, $\mathbf{m_3}$ and $\mathbf{m_4}$ are all suitable for ring closure to give the three types of crown ethers **IIIb**,**c**, **IVb**,**c** and **Vb**,**c**. It is worthy of note that although the suggested pathway appears to be plausible, some details, such as the electronic nature (ionic or free radical) for this cyclization reaction and the influence factors of the template effects for cyclization of $\mathbf{m_2}$–$\mathbf{m_4}$, still remain unclear and are worth to be further explored.

2.4. Cyclic voltammetry of cluster crown ethers ***IIIa–d***, ***IVb***,***c*** and ***Vb***,***c***

Although the electrochemical properties of some tetrahedral clusters containing MCoFeE (M = Mo, W; E = S, Se) [28], W_2FeS [29] and $M_2M'_2S_{2-4}$(M = Mo, W; M′ = Fe, Co, Ni) [30] cluster cores were reported some years ago, those of the clusters containing crown ether structural units, i.e. **IIIc**–**Vc** were just briefly reported very recently [7]. The electrochemical results obtained are summarized in Table 5. In this table the half-wave potential $E_{1/2}$ is given unless wave is irreversible(irr.). However, in the latter case an anodic peak potential E_{pa} or a cathodic one E_{pc} is listed. $E_{1/2}$ is identified with the midpoint of E_{pa} and E_{pc} of a cyclic voltammogram ($E_{pa} + E_{pc}/2$). In addition, the peak potential separation ΔE and peak current ratio I_{pc}/I_{pa} are also given when wave is reversible or quasi-reversible.

As seen from Table 6, single cluster crown ethers **IIIa**–**d** display two or three oxidation pocesses when scanning from 0.00 to + 1.50 V vs. a Standard Calomel Electrode(SCE). The first oxidation process is reversible, at least quasi-reversible. Each redox peak has a $E_{1/2}$ value of + 0.62 to + 0.66 V, a I_{pc}/I_{pa} ratio of near 1 and a redox peak separation ΔE of 81 to 91 mV. The second oxidation process is irreversible with a E_{pa} value of + 0.92 to + 1.17 V and without exhibiting a cathodic peak. The third oxidation process is also irreversible, but only observed for **IIIa** with a E_{pa} value of + 1.11 V. Furthermore, when scanning from 0.00 to − 1.60 V vs. SCE, **IIIa**–**d** each display an irreversible reduction peak with a E_{pc} value of − 1.29 to − 1.58 V. Similar electrochemical behavior was observed for double cluster crown ethers **IVb**,**c** and triple cluster crown ethers **Vb**,**c**. For example, as seen in Table 6, **IVb** exhibits a reversible oxidation peak with a $E_{1/2}$ value of + 0.65 V, an irreversible oxidation peak with $E_{pa} =$ + 1.03 V and an irreversible reduction peak with $E_{pc} =$ − 1.34 V.

2.5. Cyclic voltammetry of ***IIIa–d***, ***IVb***,***c*** and ***Vb***,***c*** in the presence of $LiPF_6$, $NaPF_6$ and KPF_6

As described above, these cluster crown ethers display one reversible redox process in the range + 0.55 to + 0.66 V. Since this process is easily attainable and could be possibly used in the molecular design of the redox-switching devices, we performed a series of cyclic voltammetry experiments with these crown ethers in the presence of $LiPF_6$, $NaPF_6$ and KPF_6. The electrochemical results of these crown ethers are summarized in Table 6.

Table 6
Electrochemical data for **IIIa**–**d**, **IVb**,**c** and **Vb**,**c** in the presence of $LiPF_6$, $NaPF_6$ and KPF_6 [a]

	Cation	$E_{1/2}$ (V)	$\Delta E_{1/2}$ (mV)		Cation	$E_{1/2}$ (V)	$\Delta E_{1/2}$ (mV)
IIIa	no	+0.618		**IVb**	no	+0.645	
	Li^+	+0.586	−32		Li^+	+0.603	−42
	Na^+	+0.593	−25		Na^+	+0.639	−6
	K^+	+0.615	−3		K^+	+0.624	−21
IIIb	no	+0.658		**IVc**	no	+0.652	
	Li^+	+0.640	−18		Li^+	+0.605	−47
	Na^+	+0.649	−9		Na^+	+0.646	−6
	K^+	+0.649	−9		K^+	+0.635	−17
IIIc	no	+0.654		**Vb**	no	+0.663	
	Li^+	+0.619	−35		Li^+	+0.622	−42
	Na^+	+0.649	−5		Na^+	+0.653	−10
	K^+	+0.645	−9		K^+	+0.657	−6
IIId	no	+0.648		**Vc**	no	+0.655	
	Li^+	+0.620	−28		Li^+	+0.620	−35
	Na^+	+0.618	−30		Na^+	+0.639	−16
	K^+	+0.635	−13		K^+	+0.647	−8

[a] Obtained in dichloromethane solution containing 0.1 M n-Bu_4NPF_6 as supporting electrolyte. Solutions were ca. 1.0×10^{-3} M in cluster crown ethers, and $LiPF_6$, $NaPF_6$ or KPF_6 was added as ca. 5.0×10^{-3} M. Potentials were determined with reference to SCE at room temperature (20 ± 1°C) and scan rate = 100 mV s^{-1}.

As far as a redox-switched system is concerned, complexation with the cation is generally shown to shift the oxidation potential of the redox-active moiety to more positive potential [31–34] and very few were found to shift cathodically [35]. Now, we have found that when addition of excess amounts of Li^+, Na^+ and K^+ cations as their PF_6^- salts to the electrochemical solutions containing **IIIa**–**d**, **IVb**,**c** and **Vb**,**c**, the oxidation potentials of their redox-active cluster cores shift cathodically. As seen in Table 6, the potentials $E_{1/2}$ for all the cation complexes of the cluster crown ethers shift to lower positive potentials compared with those of the corresponding free crown ether ligands. For example, the half-wave potential of **Vb** is 42 mV cathodical shift in the presence of $LiPF_6$. This kind of shift can be more clearly seen from the cyclic voltammograms of these cluster crown ethers and their complexes with PF_6^- salts. Fig. 4 is a representative showing a comparison of the cyclic voltammogram of **Vb** with its Li^+ complex. Apparently, such cathodic shifts for these cluster crown ethers in the presence of the alkali salts can be attributed to the slight increase in electron density around the cluster cores (possibly due to the presence of the nearby PF_6^- anions), and in turn making them easier to be oxidized.

3. Experimental

All reactions were carried out under an atmosphere of highly purified nitrogen or argon using standard Schlenk or vacuum-line techniques. Tetrahydrofuran (THF) was dried and deoxygenated by distillation from sodium–benzophenone ketyl under nitrogen. THF solutions of $Na_2[\eta^5\text{-}C_5H_4CH_2(CH_2OCH_2)_nCH_2C_5H_4\text{-}\eta^5]$ ($n = 1$ [19], $n = 2$–4 [20]), $[MoCoFe(\mu_3\text{-}S)(CO)_8]_2[\eta^5\text{-}C_5H_4CH_2(CH_2OCH_2)_nCH_2C_5H_4\text{-}\eta^5]$($n = 1$ [36], $n = 2$–4 [20]), $(\mu_3\text{-}S)FeCo_2(CO)_9$ [37] were prepared according to literature methods. $Mo(CO)_6$ and solvents used in work-up were available commercially. Dichloromethane used in CV measurements was distilled from CaH_2 and degassed. n-Bu_4NPF_6 was prepared from n-Bu_4NBr and HPF_6, whereas $LiPF_6$, $NaPF_6$ and KPF_6 were commercially available and dried by heating in vacuo. Products were separated by preparative TLC (glass plates, 20 × 25 × 0.25 cm; silica gel H, 10–40 μm). IR and ^1H-NMR spectra were recorded on a Nicolet FT-IR 5DX infrared spectrophotometer and a Bruker AC-P 200 NMR spectrometer. FAB-MS and metal analyses were carried out on a Zepspec spectrometer and a ICAP-9000 spectrometer. C/H analyses and melting point determination were performed on a Yanaco CHN Corder MT-3 analyzer and a Yanaco MP-500 apparatus, respectively.

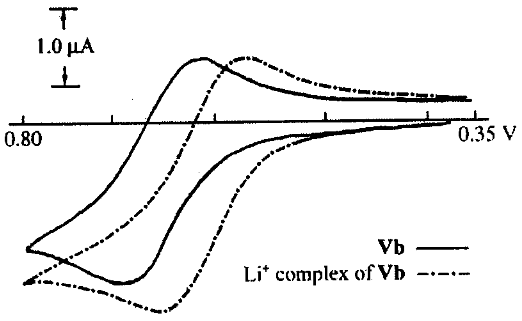

Fig. 4. A comparison between cyclic voltammograms of **Vb** and its Li^+ complex.

3.1. Preparation of $[Mo_2Fe(\mu_3\text{-}S)(CO)_7]$-$[\eta^5\text{-}C_5H_4CH_2CH_2OCH_2CH_2C_5H_4\text{-}\eta^5]$ ***(IIIa)***

A 100-ml three-necked flask equipped with a stir-bar, a serum cap and a reflux condenser topped with a N_2 inlet tube, was charged with 0.158 g (0.6 mmol) of $Mo(CO)_6$, a THF solution of ca. 0.3 mmol of $Na_2(\eta^5\text{-}C_5H_4CH_2CH_2OCH_2CH_2C_5H_4\text{-}\eta^5)$ and 10 ml of THF. The mixture was stirred and refluxed for 20 h to give $[NaMo(CO)_3]_2(\eta^5 - C_5H_4CH_2CH_2OCH_2CH_2C_5H_4 - \eta^5)$ (**Ia**). After the mixture was cooled to room temperature (r.t.), 0.340 g(0.3 mmol) of $[MoCoFe(\mu_3\text{-}S)(CO)_8]_2[\eta^5\text{-}C_5H_4CH_2CH_2OCH_2CH_2C_5H_4\text{-}\eta^5]$ (**IIa**) and 30 ml of THF were added, and the mixture was stirred and refluxed for 20 h. After removal of volatiles, the residue was extracted with CH_2Cl_2 and then the extracts were subjected to TLC using 3:2 (v/v) CH_2Cl_2/petroleum ether as eluent. From the main brown band was obtained 0.041 g (10%) of **IIIa** as a black solid. m.p. 260°C (dec). Anal. Found: C, 37.61; H, 2.25. $C_{21}H_{16}FeMo_2O_8S$ Calc.: C, 37.30; H, 2.39%. IR(KBr disk): $\nu_{C\equiv O}$ 2029vs, 1977vs, 1940vs, 1880s, 1855s, 1827vs; ν_{C-O-C} 1112m cm^{-1}. ^1H-NMR (200 MHz, $CDCl_3$): δ 2.60–3.10 (m, 4H, $2C_5H_4CH_2$), 3.58–3.70 (m, 4H, CH_2OCH_2), 4.98, 5.20 (2s, 4H, $2H^2$, $2H^5$), 5.22, 5.39 (2s, 4H, $2H^3$, $2\ H^4$).

3.2. Preparation of $[Mo_2Fe(\mu_3\text{-}S)(CO)_7]_m$-$[\eta^5\text{-}C_5H_4CH_2(CH_2OCH_2)_2CH_2C_5H_4\text{-}\eta^5]_m$ *(**IIIb**, $m = 1$; **IVb**, $m = 2$; **Vb**, $m = 3$)*

To the same equipped flask described above were added 0.264 g (1.0 mmol) of $Mo(CO)_6$, a THF solution of ca. 0.5 mmol of $Na_2[\eta^5\text{-}C_5H_4CH_2(CH_2OCH_2)_2CH_2C_5H_4\text{-}\eta^5)$ and 10 ml of THF. The mixture was stirred and refluxed for 20 h to give $[NaMo(CO)_3]_2[\eta^5\text{-}C_5H_4CH_2(CH_2OCH_2)_2\ CH_2C_5H_4\text{-}\eta^5]$ (**Ib**). After the mixture was cooled to r.t., 0.390 g (0.33 mmol) of $[MoCoFe(\mu_3\text{-}S)(CO)_8]_2[\eta^5\text{-}C_5H_4CH_2(CH_2OCH_2)_2CH_2C_5H_4\text{-}\eta^5]$ (**IIb**) and 15 ml of THF were added, and the mixture was stirred and refluxed for 50 h. After removal of volatiles, the residue was extracted with acetone and then the extracts were subjected to TLC using 30:1 (v/v) CH_2Cl_2/Et_2O as eluent. From the first brown band was obtained 0.100 g (21%) of **IIIb** as a black solid. m.p. 200°C (dec). Anal. Found: C, 38.72; H, 3.02. $C_{23}H_{20}FeMo_2O_9S$ Calc.: C, 38.36; H, 2.80%. IR (KBr disk): $\nu_{C\equiv O}$ 2028vs, 1981vs, 1957s, 1935s, 1895s, 1875s, 1821s; ν_{C-O-C} 1126m cm^{-1}. ^1H-NMR (200 MHz, $CDCl_3$): δ 2.64–3.01 (m, 4H, $2C_5H_4CH_2$), 3.64–3.75 (m, 8H, $2(CH_2OCH_2)$), 4.97, 5.20 (2s, 4H, $2H^2$, $2H^5$), 5.26, 5.30 (2s, 4H, $2H^3$, $2H^4$). From the second brown band was obtained 0.070 g (15%) of **IVb** as a brown–red solid. m.p. 57–59°C. Anal. Found: C, 38.45; H, 2.94. $C_{46}H_{40}Fe_2Mo_4O_{18}S_2$ Calc.: C, 38.36; H, 2.80%. IR (KBr disk): $\nu_{C\equiv O}$ 2034vs, 1976vs, 1888s, 1835s; ν_{C-O-C} 1110m cm^{-1}. ^1H-NMR (200 MHz, $CDCl_3$): δ 2.64 (s, 8H, $4C_5H_4CH_2$), 3.59 (s, 16H, $4(CH_2OCH_2)$), 5.15, 5.22 (2s, 16H, $4C_5H_4$). From the third brown band was obtained 0.025 g (5%) of **Vb** as a brown–red solid. m.p. 60–62°C. Anal. Found: C, 38.81; H, 3.03. $C_{69}H_{60}Fe_3Mo_6O_{27}S_3$ Calc.: C, 38.36; H, 2.80%. IR (KBr disk): $\nu_{C\equiv O}$ 2033vs, 1974vs, 1884s, 1830s; ν_{C-O-C} 1107m cm^{-1}. ^1H-NMR (200 MHz, $CDCl_3$): δ 2.64 (s, 12H, $6C_5H_4CH_2$), 3.60 (s, 24H, $6(CH_2O\ CH_2)$), 5.17, 5.21, 5.22, 5.31 (4s, 24H, $6C_5H_4$).

3.3. Preparation of $[Mo_2Fe(\mu_3\text{–}S)(CO)_7]_m$-$[\eta^5\text{–}C_5H_4CH_2(CH_2OCH_2)_3CH_2C_5H_4\text{–}\eta^5]_m$ *(**IIIc**, $m = 1$; **IVc**, $m = 2$; **Vc**, $m = 3$)*

To the flask described above were added 0.264 g (1.0 mmol) of $Mo(CO)_6$, a THF solution containing ca. 0.5 mmol of $Na_2[\eta^5\text{–}C_5H_4CH_2(CH_2OCH_2)_3CH_2C_5H_4\text{–}\eta^5]$ and 10 ml of THF. The mixture was stirred and refluxed for 20 h to give $[NaMo(CO)_3]_2[\eta^5\text{–}C_5H_4CH_2(CH_2OCH_2)_3CH_2C_5H_4\text{–}\eta^5]$ (**Ic**). Upon cooling the mixture to room temperature, 0.490 g (0.4 mmol) of $[MoCoFe(\mu_3\text{–}S)(CO)_8]_2[\eta^5\text{–}C_5H_4CH_2(CH_2OCH_2)_3CH_2C_5H_4\text{–}\eta^5]$ (**IIc**) and 30 ml of THF were added and the mixture was stirred and refluxed for 50 h. After removal of volatiles, the residue was extracted with acetone and then the extracts were subjected to TLC using 6:5 (v/v) THF/petroleum ether as eluent. From the first brown band was obtained 0.151 g (25%) of **IIIc** as a black solid. m.p. 172°C (dec). Anal. Found: C, 39.38; H, 3.11. $C_{25}H_{24}FeMo_2O_{10}S$ Calc.: C, 39.29; H, 3.17%. IR (KBr disk): $\nu_{C\equiv O}$ 2029vs, 1982vs, 1952vs, 1929vs, 1908s, 1895s, 1865s, 1840s; ν_{C-O-C} 1108m cm^{-1}. ^1H-NMR (200 MHz, $CDCl_3$): δ 2.57–2.84 (m, 4H, $2C_5H_4CH_2$), 3.47–3.79 (m, 12H, $3(CH_2OCH_2)$), 5.06 (t, 4H, $2H^2$, $2H^5$), 5.28, 5.65 (2s, 4H, $2H^3$, $2H^4$). From the second brown band was obtained 0.106 g (17%) of **IVc** as a brown–red solid. m.p. 64–66°C. Anal. Found: C, 39.57; H, 3.09. $C_{50}H_{48}Fe_2Mo_4O_{20}S_2$ Calc.: C, 39.29; H, 3.17%. IR (KBr disk): $\nu_{C\equiv O}$ 2034vs, 1975vs, 1886s, 1830s; ν_{C-O-C} 1102m cm^{-1}. ^1H-NMR (200 MHz, $CDCl_3$): δ 2.65 (s, 8H, $4C_5H_4CH_2$), 3.62 (s, 24H, $6(CH_2OCH_2)$), 5.19–5.31 (m, 16H, $4C_5H_4$). From the third brown band was obtained 0.068 g (11%) of **Vc** as a brown–red solid. m.p. 51–52°C. Anal. Found: C, 39.51; H, 3.19. $C_{75}H_{72}Fe_3Mo_6O_{30}S_3$ Calc.: C, 39.29; H, 3.17%. IR (KBr disk): $\nu_{C\equiv O}$ 2033vs, 1974vs, 1886s, 1830s; ν_{C-O-C} 1109m cm^{-1}. ^1H-NMR (200 MHz, $CDCl_3$): δ 2.63 (s, 12H, $6C_5H_4CH_2$), 3.61 (s, 36H, $9(CH_2O\ CH_2)$), 5.15–5.31 (m, 24H, $6C_5H_4$).

3.4. Preparation of $[Mo_2Fe(\mu_3\text{-}S)(CO)_7][\eta^5\text{-}C_5H_4CH_2(CH_2OCH_2)_4CH_2C_5H_4\text{-}\eta^5]$ ***(IIId)***

To the flask described above were added 0.422 g (1.6 mmol) of $Mo(CO)_6$, a THF solution containing ca. 0.8

Table 7
Crystal data and structural refinements details for **IIIa–c**

	IIIa	**IIIb**	**IIIc**
Formula	$C_{21}H_{16}FeMo_2O_8S$	$C_{23}H_{20}FeMo_2O_9S$	$C_{25}H_{24}FeMo_2O_{10}S$
Formula weight	764.25	676.14	720.19
Cryst dimensions (mm)	$0.20 \times 0.20 \times 0.30$	$0.20 \times 0.20 \times 0.30$	$0.20 \times 0.30 \times 0.30$
Crystal system	Monoclinic	Monoclinic	Monoclinic
Space group	$P2_1/n$ (no. 14)	$P2_1/c$ (no. 14)	$P2_1$ (no. 4)
a (Å)	11.670(4)	14.455(6)	11.389(2)
b (Å)	13.360(6)	11.439(2)	17.440(4)
c (Å)	14.530(5)	16.338(5)	14.726(2)
β (°)	94.53(3)	110.85(3)	109.17(1)
V (Å^3)	2258(1)	2524(1)	2762.6(9)
Z	4	4	4
D_{calc} (g cm^{-3})	1.988	1.895	1.837
F(000)	1328	1424	1520
μ (Mo–K$_\alpha$) (cm^{-1})	18.63	16.76	15.16
Temperature (K)	293	293	296
Wavelength (Å)	0.71069	0.71069	0.71069
Scan type	ω–2θ	ω–2θ	ω–2θ
$2\theta_{max}$ (°)	50.0	49.9	53.9
No. of observns, n	2732	2933	5994
No. of variables, p	299	326	747
R	0.041	0.029	0.045
R_w	0.050	0.035	0.054
Goodness-of-fit	1.60	1.32	1.54
Largest difference peak and hole (e Å^{-3})	0.56 and −0.68	0.41 and −0.70	1.07 and −2.38

mmol of $Na_2[\eta^5\text{-}C_5H_4CH_2(CH_2OCH_2)_4CH_2C_5H_4\text{-}\eta^5]$ and 20 ml of THF. The mixture was stirred and refluxed for 20 h to give $[NaMo(CO)_3]_2[\eta^5\text{-}C_5H_4(CH_2OCH_2)_4CH_2C_5H_4\text{-}\eta^5]$ (**Id**). Upon cooling the mixture to r.t., 0.633 g (0.5 mmol) of $[MoCoFe(\mu_3\text{-}S)(CO)_8]_2[\eta^5\text{-}C_5H_4CH_2(CH_2O\ CH_2)_4CH_2C_5H_4\text{-}\eta^5]$ (**IId**) and 20 ml of THF were added and the mixture was stirred and refluxed for 50 h. Solvent was removed under vacuum to give a residue. The residue was extracted with acctone and then the extracts were subjected to TLC using 30:1 (v/v) CH_2Cl_2/THF as eluent. From the main brown band was obtained 0.140 g (17%) of **IIId** as a brown–red solid. m.p. 100–101°C. Anal. Found: C, 39.81; H, 3.24. $C_{27}H_{28}FeMo_2O_{11}S$ Calc.: C, 40.12; H, 3.49%. IR (KBr disk): $\nu_{C\equiv O}$ 2031vs, 1976vs, 1943vs, 1914s, 1883s, 1836vs; ν_{C-O-C} 1119m cm^{-1}. ^{1}H-NMR (200 MHz, $CDCl_3$): δ 2.63–2.71 (m, 4H, $2C_5H_4CH_2$), 3.58–3.68 (m, 16H, $4(CH_2OCH_2)$), 5.16 (s, 4H, $2H^2$, $2H^5$), 5.20, 5.42 (2s, 4H, $2H^3$, $2H^4$).

3.5. X-ray structure determinations of ***IIIa–c***

Single-crystals of **IIIa**, **IIIb and IIIc** suitable for X-ray diffraction analyses were grown by slow evaporation of their CH_2Cl_2/hexane solutions at about 4°C. Each crystal was mounted on a Rigaku AFC7R or an Enraf-Nonius CAD4 diffractometer with a graphite monochromator with MoKα radiation ($\lambda = 0.71069$Å). Details of the crystal data, data collections and structure refinements are summarized in Table 7. The structures were solved by direct methods and expanded by Fourier techniques. The final refinements were accomplished by the full-matrix least-squares method with anisotropic thermal parameters for non-hydrogen atoms. The calculations for **IIIa–c** were performed using the TEXSAN crystallographic software package of the Molecular Structure Corporation.

3.6. Cyclic voltammetry measurements of ***IIIa–d***, ***IVb***,***c*** and ***Vb***,***c***

Cyclic voltammetry measurements were performed using a BAS-100B electrochemical analyzer and were carried out in dichloromethane solution containing 0.1 M n-Bu_4NPF_6 using a platinum working electrode ($\varphi = 1$ mm) and a platinum wire counter electrode, with ferrocene, $E_{1/2} = 0.41$–0.42 V, as internal reference. All potential values are quoted relative to SCE.

The dichloromethane solution, ca. 1.0×10^{-3} M in cluster compound or ca. 5.0×10^{-3} M in $LiPF_6$, $NaPF_6$ or KPF_6, was placed in a single-compartment electrochemical cell and degassed by bubbling with argon for 5 min before measurement. An argon atmosphere was continuously maintained above the solution while the experiments were in progress. The platinum working electrode surface was polished with 0.05 μm alumina, sonicated in distilled water, and air-dried immediately before use.

4. Supplementary material

Crystallographic data for the structural analysis have been deposited with the Cambridge Crystallographic Data Centre, CCDC no. 150514 for **IIIa**, CCDC no. 150515 for **IIIb** and CCDC no. 150516 for **IIIc**. Copies of this information may be obtained from The Director, CCDC, 12 Union Road, Cambridge, CB2 1EZ, UK (fax: +44-1233-336033; e-mail: deposit@ccdc.cam.ac.uk or www: http://www.ccdc.cam.ac.uk).

Acknowledgements

We are grateful to the National Natural Sience Foundation of China, Laboratory of Organometallic Chemistry and State Key Laboratory of Structural Chemistry for financial support of this work.

References

[1] C.J. Pederson, J. Am. Chem. Soc. 89 (1967) 7017.

[2] G.W. Gokel, Crown Ethers and Cryptands, Monographs in Supramolecular Chemistry, Royal Society of Chemistry, Cambridge, UK, 1991.

[3] B. Dietrich, P. Viout, J.-M. Lehn, Macrocyclic Chemistry, VCH, Weinheim, 1993.

[4] F. Vögtle, Supramolecular Chemistry, An Introduction, Wiley, Chichester, UK, 1991.

[5] J.-M. Lehn, Supramolecular Chemistry, Concepts and Perspectives, VCH, Weinheim, 1995.

[6] F.C.J.M. van Veggel, W. Verboom, D.N. Reinhoudt, Chem. Rev. 94 (1994) 279.

[7] L.-C. Song, D.-S. Guo, Q.-M. Hu, X.-Y. Huang, Organometallics 19 (2000) 960.

[8] (a) N.D. Lowe, C.D. Garner, J. Chem. Soc. Dalton Trans. (1993) 2197. (b) N.D. Lowe, C.D. Garner, J. Chem. Soc. Dalton Trans. (1993) 3333.

[9] E. Solari, W. Lesueur, A. Klose, K. Schenk, C. Floriani, A. Chiesi-Villa, C. Rizzoli, J. Chem. Soc. Chem. Commun. (1996) 807.

[10] M. Moran, C.M. Casado, I. Cuadrado, J. Losada, Inorg. Chim. Acta 185 (1991) 33.

[11] E. Fu, J. Granell, M.L.H. Green, V.J. Lowe, S.R. Marder, G.C. Saunders, M. Tuddenham, J. Organomet. Chem. 355 (1988) 205.

[12] H. Plenio, R. Diodone, J. Org. Chem. 58 (1993) 6650.

[13] H. Plenio, D. Burth, Organometallics 15 (1996) 1151.

[14] S. Bélanger, M. Gilbertson, D.I. Yoon, C.L. Stern, X. Dang, J.T. Hupp, J. Chem. Soc. Dalton Trans. (1999) 3407.

[15] (a) T. Izumi, T. Tezuka, S. Yusa, A. Kasahara, Bull. Chem. Soc. Jpn. 57 (1984) 2435. (b) S. Akabori, H. Fukuda, Y. Habata, M. Sato, S. Ebine, Chem. Lett. (1982) 1393. (c) T. Saji, Chem. Lett. (1986) 275. (d) M.C. Grossel, M.R. Goldspink, J.A. Hriljac, S.C. Weston, Organometallics 10 (1991) 851. (e) M.C. Grossel, M.R. Goldspink, J.P. Knychala, A.K. Cheetham, J.A. Hriljac, J. Organomet. Chem. 352 (1988) C13. (f) M. Sato, M. Kubo, S. Ebine, S. Akobori, Tetrahedron Lett. 23 (1982) 185. (g) H. Plenio, C. Aberle, Angew. Chem. Int. Ed. Engl. 37 (1998) 1397. (h) G.C. Dol, P.C.J. Kamer, F. Hartl, P.W.N.M. van Leeuwen, R.J.M. Nolte, J. Chem. Soc. Dalton Trans. (1998) 2083. (i) M. Herberhold, H.-D. Brendel, A. Hofmann, B. Hofmann, W. Milius, J. Organomet. Chem. 556 (1998) 173. (j) J.C. Medina, T.T. Goodnow, S. Bott, J.L. Atwood, A.E. Kaifer, G.W. Gokel, J. Chem. Soc. Chem. Commun. (1991) 290. (k) J.C. Medina, T.T. Goodnow, M.T. Rojas, J.L. Atwood, B.C. Lynn, A.E. Kaifer, G.W. Gokel, J. Am. Chem. Soc. 114 (1992) 10583.

[16] (a) P.D. Beer, A.D. Keefe, H. Sikanyika, C. Blackburn, J.F. McAleer, J. Chem. Soc. Dalton Trans. (1990) 3289. (b) T. Izumi, S. Murakami, A. Kasahara, Bull. Chem. Soc. Jpn. 61 (1988) 3565.

[17] (a) P.D. Beer, Acc. Chem. Res. 31 (1998) 71. (b) P.D. Beer, A.D. Keefe, J. Organomet. Chem. 375 (1989) C40.

[18] (a) J.R. Farrell, C.A. Mirkin, L.M. Liable-Sands, A.L. Rheingold, J. Am. Chem. Soc. 120 (1998) 11834. (b) J.R. Farrell, C.A. Mirkin, I.A. Guzei, L.M. Liable-Sands, A.L. Rheingold, Angew. Chem. Int. Ed. Engl. 37 (1998) 465.

[19] L.-C. Song, Y.-B. Dong, Q.-M. Hu, J. Sun, Organometallics 15 (1996) 1954.

[20] L.-C. Song, D.-S. Guo, Q.-M. Hu, J. Chem. Res. (S) (1999) 516.

[21] (a) L.-C. Song, J.-Y. Shen, Q.-M. Hu, R.-J. Wang, H.-G. Wang, Organometallics 12 (1993) 408. (b) L.-C. Song, J.-Y. Shen, Q.-M. Hu, X.-Y. Huang, Organometallics 14 (1995) 98. (c) L.-C. Song, Y.-B. Dong, Q.-M. Hu, X.-Y. Huang, J. Sun, Organometallics 16 (1997) 4540. (d) L.-C. Song, H.-T. Fan, Q.-M. Hu, X.-D. Qin, W.-F. Zhu, Y. Chen, J. Sun, Organometallics 17 (1998) 3454. (e) L.-C. Song, Y.-B. Dong, Q.-M. Hu, W.-Q. Gao, D.-S. Guo, P.-C. Liu, X.-Y. Huang, J. Sun, Organometallics 18 (1999) 2168.

[22] F. Richter, E. Roland, H. Vahrenkamp, Chem. Ber. 117 (1984) 2429.

[23] L.-C. Song, J.-Y. Shen, Q.-M. Hu, X.-D. Qin, Polyhedron 14 (1995) 2079.

[24] D.M. Curtis, K.R. Han, W.M. Butler, Inorg. Chem. 19 (1980) 2096.

[25] R. Hoffmann, Angew. Chem. Int. Ed. Engl. 21 (1982) 711.

[26] (a) H. Vahrenkamp, Comments Inorg. Chem. 4 (1985) 253. (b) L.-C. Song, J.-Y. Shen, Q.-M. Hu, B.-S. Han, R.-J. Wang, H.-G. Wang, Inorg. Chim. Acta 219 (1994) 93. (c) L.-C. Song, Y.-B. Dong, Q.-M. Hu, Y.-K. Li, J. Sun, Polyhedron 17 (1998) 1579. (d) L.-C. Song, Y.-K. Li, Q.-M. Hu, J. Sun, J. Coord. Chem. 45 (1998) 1.

[27] (a) S. Anderson, H.L. Anderson, J.K.M. Sanders, Acc. Chem. Res. 26 (1993) 469. (b) R. Hoss, F. Vögtle, Angew. Chem. Int. Ed. Engl. 33 (1994) 375. (c) D.H. Busch, N.A. Stephenson, Coord. Chem. Rev. 100 (1990) 119.

[28] U. Honrath, H.Z. Vahrenkamp, Naturforsch. Teil B 39 (1984) 545.

[29] P.D. Williams, M.D. Curtis, J. Organomet. Chem. 352 (1988) 169.

[30] M.D. Curtis, P.D. Williams, W.M. Butler, Inorg. Chem. 27 (1988) 2853.

[31] P.D. Beer, Chem. Soc. Rev. 18 (1989) 409.

[32] C.D. Hall, N.W. Sharpe, I.P. Danks, Y.P. Sang, J. Chem. Soc. Chem. Commun. (1989) 419.

[33] C.D. Hall, S.Y.F. Chu, J. Organomet. Chem. 498 (1995) 221.

[34] H. Plenio, C. Aberle, Chem. Commun. (1998) 2697.

[35] C.D. Hall, N. Sachsinger, S.C. Nyburg, J.W. Steed, J. Organomet. Chem. 561 (1998) 209.

[36] L.-C. Song, D.-S. Guo, Y.-B. Dong, Transition Met. Chem. 25 (2000) 37.

[37] M. Cowie, R.L. DeKock, T.R. Wagenmaker, D. Seyferth, R.S. Henderson, M.K. Gallagher, Organometallics 8 (1989) 119.